ACS OMEGA

http://pubs.acs.org/journal/acsodf

Article

Discerning the Metal Doping Effect on Surface Redox and Acidic Properties in a MoVTeNbO$_x$ for Propa(e)ne Oxidation

Roberto Quintana-Solórzano,* Isidro Mejía-Centeno, Hector Armendáriz-Herrera, Joel Ramírez-Salgado, Andrea Rodríguez-Hernandez, Maria de Lourdes Guzmán-Castillo, Jose M. Lopez Nieto, and Jaime S. Valente

Cite This: *ACS Omega* 2021, 6, 15279−15291

Read Online

ACCESS | Metrics & More | Article Recommendations | Supporting Information

ABSTRACT: Adding a small quantity of K or Bi to a MoVTeNbO$_x$ via impregnation with inorganic solutions modifies its surface acid and redox properties and its catalytic performance in propa(e)ne partial oxidation to acrylic acid (AA) without detriment to its pristine crystalline structure. Bi-doping encourages propane oxydehydrogenation to propene, thus enlarging the net production rate of AA up to 35% more. The easier propane activation/higher AA production over the Bi-doped catalyst is ascribed to its higher content of surface V leading to a larger amount of total V^{5+} species, the isolation site effect of NbO$_x$ species on V, and its higher Lewis acidity. K-doping does not affect propane oxydehydrogenation to propene but mainly acts over propene once formed, also increasing AA to a similar extent as Bi-doping. Although K-doping lowers propene conversion, it is converted more selectively to acrylic acid owing to its reduced Brønsted acidity and the presence of more Mo^{6+} species, thereby favoring propene transformation via the π-allylic species route producing acrylic acid over that forming acetic acid and CO$_x$ via acetone oxidation and that yielding directly CO$_x$.

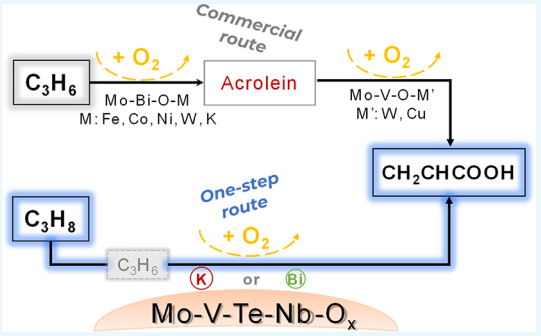

1. INTRODUCTION

With the global market growing at a rate of ca. 4% per year, acrylic acid is a high-value intermediate compound used for manufacturing paints, acrylic esters, polymers, etc. To date, the principal commercial process to produce acrylic acid is the two-step propene partial oxidation in the vapor phase.[1] It comprises two fixed-bed reactors in series requiring also two distinct and relatively complex catalyst formulations using air as the oxygen source: propene oxidizes to acrolein from 310 to 330 °C in reactor one, and acrolein transforms to acrylic acid between 210 and 235 °C in reactor two.[2−5] The high overall propene conversion (ca. 95%) and acrylic acid selectivity (ca. 90%) support the profitability of this exothermic process.[2]

For years, there has been a worldwide interest in developing a one-step catalytic technology to yield acrylic acid starting from propene and, preferably, from propane that is naturally available, more abundant, and less demanded and expensive compared to propene.[2] This one-step route encompasses a relatively complex chemistry, the desired pathway corresponding to the sequence propane−propene−acrolein−acrylic acid[5,6] wherein propane oxydehydrogenation to propene is suggested as the rate determining step.[3,7] Besides this pathway, other reaction routes, which are even more favorable thermodynamically and lead to other oxygenate compounds (acetone, acetic acid, etc.) and deep oxidation products (CO$_x$), have been identified.[4−10] Given that complexity, a multifunctional catalyst with the ability to oxydehydrogenate propane to propene and then insert oxygen atoms to form acrolein and finally acrylic acid, thus preventing unwanted oxygenate compounds and CO$_x$, is required. This implies the concomitant participation of various catalytic functions along with well-balanced reduction−oxidation properties of the constituting metals and adequate acidic properties for such a complex redox cycle.

While developing catalysts for propane (amm)oxidation, a key turning point is attributed to Mitsubishi Chem. Co. that produced acrylic acid[11−13] or acrylonitrile[14−17] via direct oxidation routes over MoVTeNbO$_x$. So far, Mo-V-based catalysts, which contain other transition metals such as Te, Nb, or Sb and are constituted of two principal crystalline phases, i.e., M1 and M2, are identified as the most successful catalysts to oxidize propane to acrylic acid.[18−22] Containing V^{5+} as paraffin activating species, orthorhombic phase M1 is involved in activity and selectivity, while, lacking V^{5+} species, phase M2 would improve selectivity. Although catalysts

Received: March 24, 2021
Accepted: May 18, 2021
Published: June 2, 2021

containing only phase M1 exhibit a good combined performance in propane conversion and acrylic acid selectivity,[3,22] they perform better when phases M1 and M2 operate synergistically.[23−25] Acrylic acid selectivity can be further enlarged by adjusting reaction conditions, e.g., adding water to the reaction mixture,[26−28] or by recycling unconverted propane.[29]

Luo et al.[8] proposed the presence of two active sites in a $MoV_{0.3}Te_{0.23}Nb_{0.12}$ mixed oxide: (i) one participating in propane oxydehydrogenation to propene, which is then oxidized to an allyl alcohol, acrolein, and acrylic acid, and (ii) a second oxidizing propene to 2-propanol that rapidly reconverts to acetone, which then oxidizes to acetic acid and CO_x. Others suggested that $MoVTeNbO_x$ contain, at least, three catalytic oxidation functions, to wit, one site promoting propane conversion to propene, a second site catalyzing the allylic oxidation of propene to acrolein, and a third site oxidizing acrolein to acrylic acid. López Nieto et al.[20,30−33] stated the presence of a propane activation site (V^{5+} sites), a H-abstracting site (Te^{4+} or Sb^{3+}), and an O-insertion site (Mo^{6+}) in a well-defined host structure, i.e., $Te_2M_{20}O_{57}$ (with M = Mo, V, Nb) or $(SbO)_2M_{20}O_{56}$ (with M = Mo, V, Nb).

The catalytic properties of crystalline phases M1 and M2 can be tuned by adding promoters and/or substituting selected elements aimed to selectively route propane or propene conversion to acrylic acid.[3,31−38] Grasselli et al.[3] separately doped phases M1 and M2 with low amounts of P, reporting that acrylic acid yield increased from 24 to 33% when converting 47% of fed propene over a catalyst with a P to Mo nominal ratio of 0.005. They concluded that P−V and P−Mo electronic interactions along with the acidic nature of P enhanced propene chemisorption, thus promoting its transformation to acrylic acid via acrolein. Grasselli et al.[35] also investigated the influence of adding several elements to modify the acidic (P, B, and W), basic (Cs), and redox (Cu) properties of crystalline phases M1 and M2 separately on propane and propene conversion to acrylic acid; Cu-doping did not alter their base performance, Cs-doping negatively affected acrylic acid formation, while P-, B-, or W-doping improved acrylic acid production from 2 to 10%.

After adding alkali metals to $MoVSbO_x$, López Nieto et al.[32−34] found an improvement in acrylic acid selectivity, which was attributed to a decline in the catalyst's surface acidity. They suggested that a π-bonded propene species was formed on Brønsted acid sites, yielding an isopropoxide species that may follow a pathway to CO_x. K was used to modify the selectivity of crystalline phases M1 and M2 composing $MoV(Te/Sb)(Nb)O_x$.[32,39] Selectivity to acrylic acid increased from 15 to 40% to the detriment of that to acetic acid when doping $MoVSbO_x$ with K, without detecting changes in crystalline structure.[32] This confirmed that K changes the catalyst's surface acidity,[39] producing an improvement in acrylic acid selectivity due to a partial elimination of Brønsted sites. Besides, the relatively low acrylic acid selectivity for $MoVTeO_x$ and $MoVSbO_x$ has been reasoned in terms of the presence of Brønsted and Lewis acid sites, whose amount decreased or even disappeared over Nb-$MoVTeO_x$ or K-$MoVSbO_x$ systems.[31−34,40,41]

Ishchenko et al.[36−38] investigated the effect of incorporating K and Bi ions to phase M1 of $MoVTeNbO_x$ on ethane oxydehydrogenation to ethylene (ODHE). Because of a diminution in the fraction of active (001) surface plane and the relative content of V^{5+} species, K addition, however, reduced the catalyst's activity.[36] The addition of Bi ions in moderate amounts (Bi/Mo = 0.015−0.025), in contrast, increased both the catalyst's activity and stability when operating at severe reducing conditions as this metal would incorporate into the six-membered channels of phase M1 hampering Te ion segregation and loss under severe reaction conditions.[37,38] Lazareva et al. claimed that Bi addition increased $MoVNbTeO_x$ stability, maintaining its catalytic performance in ODHE[36−38] and propane oxidation to acrylic acid;[42] over a calcined $MoVTeNbO_x$ impregnated with a Bi-containing organic solution, an acrylic acid yield as high as 48% was achieved. Bi ion addition to $MoVTeNbO_x$, nonetheless, led to a decrease in the amount of phase M1 from ca. 98 to 70−80 wt %, which transformed to phase M2.[37,42]

Based on the above, the propane to acrylic acid single-step oxidation process remains as an attractive subject of research, and despite the existence of reports on the field, additional investigation has value in the way to develop more efficient catalytic materials for a more profitable process scenario. This work centers on understanding how changes in surface acid and redox properties of a $MoVTeNbO_x$, measured via FT-IR spectra of adsorbed/desorbed pyridine and XPS, after doping with K or Bi impact propane oxidation to acrylic acid. Although different in nature, Bi and K have been effectively used as dopants. With a similar atomic radius to Te (0.146 vs 0.137 nm) and five valence electrons, Bi is a post-transition metal that is expected to have a role in activity and stability, which is important due to the exothermicity of oxidation reactions. Having one valence electron and a larger atomic radius than Bi (0.231 vs 0.146 nm) and being less electronegative than Bi, K is an alkali metal that would interact with surface metallic species and neutralize acid sites rather than produce structural alterations in the catalyst. The said catalyst's promoting effect has been mostly focused on ODHE[36−38] or propane ammoxidation, with results that are still subject to discussion. Also, aimed at breaking down the role of the two said doping metals in the propane to acrylic acid pathway, which involves propene in a first stage, as well as product distribution in detail, independent experiments feeding propane and propene are carried out.

2. EXPERIMENTAL PROCEDURES

2.1. Synthesis of Catalysts. A $MoVTeNbO_x$ having a nominal Mo/V/Te/Nb molar proportion of 1.0/0.24/0.24/0.18 was prepared following the procedure comprising these steps (vide ref 43 for details): (i) prepare under continuous stirring at 80 °C an aqueous solution containing ammonium heptamolybdate tetrahydrate, telluric acid, and ammonium metavanadate (solution A); (ii) prepare under continuous stirring at 80 °C another aqueous solution containing niobium oxalate and oxalic acid (solution B); (iii) slowly add solution B into solution A under continuous vigorous stirring to produce a slurry; (iv) cool the slurry to room temperature and adjust the pH to 2.5 using 1 M nitric acid solution; (v) rotaevaporate the slurry at 50 °C and 27 kPa to obtain a solid and then dry the solid overnight at 100 °C; and (vi) activate at 600 °C for 2 h under a flow of nitrogen the dried solid to be used as catalyst. The resulting material corresponds to the base catalyst denoted as Cat-Te. With the aim of improving its catalytic properties, Cat-Te was doped with K or Bi via wet impregnation using nitrate solutions of the metal, as follows: (i) dissolve the metallic salt in deionized water; (ii) add 2 g of the solid activated material into the metallic solution, keeping the resulting suspension under stirring for 3 h at room temper-

https://doi.org/10.1021/acsomega.1c01591
ACS Omega 2021, 6, 15279−15291

ature; (iii) evaporate the aqueous fraction of the suspension in a rotavapor at 60 °C and 9.6 kPa; (iv) dry the solid recovered at 120 °C; and (v) treat the dried solid with nitrogen at 500 °C for 2 h. The resulting materials were denoted as Cat-Te007K and Cat-Te007Bi, with the number meaning the nominal Me/Mo (Me = K or Bi) molar ratio.

2.2. Characterization of Catalysts. *2.2.1. Inductively Coupled Plasma Atomic Emission Spectrometry (ICP-AES).* The elementary composition of catalyst samples was verified by performing the analyses in a Perkin Elmer Mod OPTIMA 3200 Dual Vision equipment in accordance with the EPA-6010C method.

2.2.2. X-ray Diffraction (XRD). For the analyses, catalyst samples were packed in a glass holder. The XRD patterns were then recorded on a Siemens D-5005 diffractometer using a $\theta-\theta$ configuration and a graphite monochromatized secondary beam. Diffraction intensities were measured from 4 to 60° with a 2θ step equal to 0.02° for 8 s per point using Cu $K_{\alpha 1,2}$ radiation with a wavelength of 1.5418 Å at 40 V and 40 mA.

2.2.3. X-ray Photoelectron Spectroscopy (XPS). Analyses of catalyst samples were performed in a Thermo VG Scientific Escalab 250 spectrometer equipped with a channeltron detector. The X-ray radiation source was monochromatic of Al Kα (1486.6 eV) operating at 150 W (15 kV, 5.5 mA). Survey spectra and element regions were recorded defining a 150 and 20 eV pass energy to have high resolution. The operating conditions were 20 °C and 3×10^{-9} kPa. The C−C signal from adventitious carbon (C 1s) at 284.8 ± 0.02 eV was used as an internal reference. Data acquisition and processing were done in the Avantage software version 5.982. Fitted defining a Smart−Shirley background, the spectra were deconvoluted using Gaussian (70%) plus Lorentzian (30%) product functions with set values of full width at half-maximum (FWHM) for each peak shape.

2.2.4. Fourier Transform Infrared (FT-IR) Pyridine Adsorption−Desorption. Catalyst samples were analyzed to determine the nature, density and strength of their surface acid sites. The FT-IR spectra were recorded in a Nicolet model 170 SX spectrometer. Prior to being analyzed, the catalyst powder was pressed into self-supporting wafers and then pretreated in a Pyrex glass gas cell with CaF_2 windows by outgassing at 400 °C under vacuum at 1×10^{-7} kPa. Upon pretreatment, the samples were exposed to pyridine vapor for 0.33 h by breaking the capillary tube containing 1×10^{-3} cm^3 of this substance. After pyridine adsorption, the infrared spectra were registered at varying temperatures from 100 to 300 °C for a gradual desorption of the adsorbed pyridine.

2.3. Catalytic Testing. *2.3.1. Experimental Setup.* Catalytic experiments were carried out at the laboratory scale in a fixed-bed tubular reactor made of quartz having an internal diameter of 1.4×10^{-2} m and a length of 4.0×10^{-2} m, which was operated at isothermal and isobaric conditions. The reactor was packed with 0.80 g of the catalyst diluted with 3.2 g of SiC, the latter used for increasing the effective thermal conductivity of the bed. The catalyst and diluent were sieved for a particle size ranging from 149 to 250 μm prior to being loaded into the reactor. Two sets of independent experiments were performed, feeding propane in the first one and propene in the second one and using the same reactor inlet composition in both. The reaction mixture consisted of propane or propene, oxygen, nitrogen, and deionized water (ca. 20 MΩ·cm). Supplied by PraxAir Mexico, said gases were 99 vol % min. purity. The inlet flow rate of the gases was quantified with Brooks 5850i series thermal mass flow controllers (MFCs), while water flow was dosed by using a high-precision syringe pump. Once vaporized at 150 °C, water was blended with a stream containing propane or propene, oxygen, as well as nitrogen, and the resulting mixture was then directed to the reactor. To determine the composition of the reactor effluent after commencing the reaction, periodic online analyses were carried out in an Agilent 7890A Gas Chromatograph with a configuration comprising three detectors, to wit, two flame ionization detectors (FID) and a thermal conductivity detector (TCD), two multiport valves, and four capillary columns (vide ref 27 for details).

2.3.2. Reaction Conditions. A feed proportion propane (or propene)/oxygen/water/nitrogen equal to 1.0/2.2/3.7/17 (mole basis) was used, operating the reactor at 100 kPa, temperature from 300 to 420 °C, and space-time (W/F°) between 55 and 110 g_{cat} $h(mol_{propa(e)ne})^{-1}$. For brevity's sake, the word "propa(e)ne" is systematically used in this work to denote "propane or propene". As propa(e)ne and oxygen produce potentially flammable mixtures, it must be diluted with a relatively large amount of inert. Nitrogen was used as the diluent and served as the internal standard for mass balance purposes. Note that in the commercial process to produce acrylic acid from propene, the reactor feed contains a large amount of nitrogen as air is used as the source of oxygen. As water was also added to the reactor, the reaction mixture is a highly diluted stream where the concentration of nitrogen plus water is larger than 80 mol %: this is a technical requirement considering the aspects of safety (flammability), reactor thermal stability, productivity, coke formation, etc.[44,45]

The potential of flammability (PF) of the reaction mixture for the catalytic experiments was assessed. As both hydrocarbons possess, as pure substances, similar flammability levels, the PF was verified only for the stream containing propane at the most severe reaction conditions in temperature (420 °C). Based on a ternary plot constructed using the methodology reported in ref 46, the said reaction mixture composition was found to be out of a flammable region. Likewise, carried out at 100 kPa over a bed consisting only of SiC, blank experiments feeding propene at 380 °C and propane at 420 °C confirmed that neither of them was converted in the absence of the catalyst.

2.3.3. Catalytic Responses. The values of hydrocarbon conversion and selectivity or yield to products were calculated to quantify the catalysts' behavior. Given on a carbon basis, these catalytic responses were obtained after reaching steady state in the catalysts' operation. For instance, propa(e)ne conversion, acrylic acid selectivity, and CO yield were computed by eqs 1, 2, and 3, respectively.

$$X_{C,propa(e)ne} = \frac{G^{o}_{C,propa(e)ne} - G_{C,propa(e)ne}}{G^{o}_{C,propa(e)ne}} \times 100 \quad (1)$$

$$S_{C,acrylic\ acid} = \frac{G_{C,acrylic\ acid}}{G^{o}_{C,propa(e)ne} - G_{C,propa(e)ne}} \times 100 \quad (2)$$

$$Y_{C,CO} = \frac{G_{C,CO}}{G^{o}_{C,propa(e)ne}} \times 100 \quad (3)$$

$G^{o}_{C,\ propa(e)ne}$ is the mass flow rate of carbon in propa(e)ne at the reactor inlet, whereas $G_{C,propa(e)ne}$, $G_{C,acrylic\ acid}$, and $G_{C,CO}$ are the mass flow rate of carbon in propa(e)ne, acrylic acid,

https://doi.org/10.1021/acsomega.1c01591
ACS Omega 2021, 6, 15279−15291

Table 1. Metallic Composition Obtained via ICP-AES and XPS Analyses of the Three Catalyst Samples[a]

catalyst sample	V/Mo	Te/Mo	Nb/Mo	K/Mo	Bi/Mo	V^{5+}/V	Mo^{5+}/Mo	$Nb(NbO_x)/Nb(M1)$
					ICP-AES, at. ratio			
Cat-Te	0.19	0.18	0.10	0.0	0.0	-	-	-
Cat-Te007K	-	-	-	0.007		-	-	-
Cat-Te007Bi	-	-	-	-	0.007	-	-	-
					XPS, at. ratio			
Cat-Te	0.09	0.32	0.18	0.0	0.0	0.41	0.09	0.39
Cat-Te007K	0.09	0.23	0.19	0.006	0.0	0.72	0.04	0.30
Cat-Te007Bi	0.19	0.17	0.38	0.0	0.05	0.39	0.11	0.59

[a]Values reported correspond to the atomic ratio (at. ratio) of metals and/or metallic species.

and CO, respectively, at the reactor outlet. The flow rates of gaseous species at the reactor entrance were obtained from the volumetric flow rates quantified by the MFCs. The carbon-based reactor outlet flow rate of species *i* was quantified indirectly via the so-called internal standard method incorporating the number of carbon atoms in the molecule as well as the atomic mass of carbon, as explained in detail in ref 27.

3. RESULTS AND DISCUSSION

3.1. Characterization of Catalysts. *3.1.1. Chemical Composition via ICP-AES.* The base catalyst was subjected to ICP-AES analysis to determine the content of Mo, V, Te, and Nb, while the catalysts doped with Me were only analyzed for K and Bi. The composition of the catalyst Cat-Te was 48.1 wt % of Mo, 5.1 wt % of V, 10.1 wt % of Te, and 4.5 wt % of Nb, giving a real molar distribution related to Mo equal to $MoV_{0.194}Te_{0.183}Nb_{0.096}$, while for the catalyst samples doped with K or Bi, the real molar ratio of Me (Me = K or Bi) to Mo was very similar for both Cat-Te007K and Cat-Te007Bi, amounting to 0.007 (Table 1). The composition results from XPS analyses were also included in Table 1 and will be discussed in a further section.

3.1.2. X-ray Diffraction. Figure 1 displays the XRD patterns of the catalyst samples investigated in this work. The

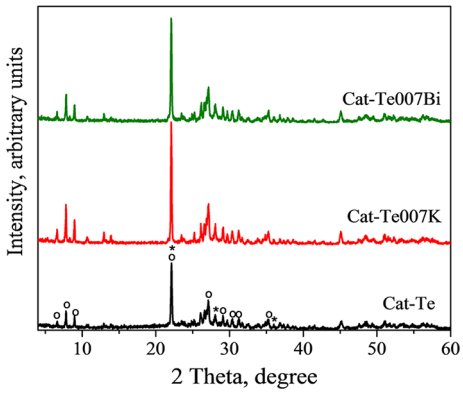

Figure 1. XRD diffraction patterns of the catalyst samples coded as Cat-Te, Cat-Te007K, and Cat-Te007Bi. The crystalline phases identified in the solids were denoted as follows: (circles) M1 and (asterisks) M2.

diffraction peaks located at 2θ equal to 7.8, 8.9, 22.1, 27.1, 39.3, 30.5, and 35.4° indicate the presence of crystalline phase M1 (ICDD, PDF 01-073-7574). With peaks situated at 2θ equal to 22.2, 28.2, 36.2, 45, and 50° (ICDD, PDF 00-057-1099), crystalline phase M2 also constituted the catalysts. Previously,[47] a Rietveld refinement of the XRD spectra indicated that phase M1 was the main constituent of the base catalyst (95 wt %), with the rest basically consisting of phase M2. Interestingly, the catalysts doped with K (Cat-Te007K) or Bi (Cat-Te007Bi) did not exhibit any evident structural deviation in comparison to the pattern of the base catalyst, while other phases containing Bi or K were not detected (Figure 1), contrasting with the notable decrease of phase M1 detected in ref 42.

3.1.3. XPS. Figure 2 presents the $V2p_{3/2}$, $Mo3d_{5/2}$, $Nb5d_{5/2}$, and $Te3d_{5/2}$ XPS spectra for the base catalyst (Cat-Te) as well as the materials doped with K (Cat-Te007K) or Bi (Cat-Te007Bi). The relative amount of metal (Mo, V, Te, and Nb) species with different oxidation states is also depicted in Figure 2. Figure 3 shows the $K2p_{3/2}$ and $Bi4f_{7/2}$ XPS spectra for (K or Bi) doped catalysts, while Table 1 summarizes values of the corresponding atomic surface metallic composition. In agreement with other reports[48,49] stating that the amount of surface V located on MoVTe(Sb)(Nb) mixed oxides is smaller compared to its counterpart in the bulk, the surface V on Cat-Te and Cat-Te007K was practically half (V/Mo = 0.09 at. ratio in both cases) of the V in the bulk (V/Mo = 0.19 at. ratio). In contrast, the quantity of V on the surface and in the bulk was practically the same for catalyst Cat-Te007Bi (V/Mo = 0.19 at. ratio). For the three catalyst samples, in turn, the surface content of Nb, namely, Nb/Mo = 0.18, 0.19, and 0.38 at. ratio for Cat-Te, Cat-Te007K, and Cat-Te007Bi, respectively, was consistently larger compared to that in the bulk (Nb/Mo = 0.10 at. ratio). The concentration of Te on the surface, Te/Mo =0.32 at. ratio for Cat-Te and 0.23 at. ratio for Cat-Te007K, was also higher in comparison to its counterpart in the bulk (0.18 at. ratio), while the Te/Mo at. ratio in the bulk and on the surface was rather similar for Cat-Te007Bi (0.18 vs 0.17, Table 1). Concerning doping metals, the amount of surface Bi was notably higher than that in the bulk (Bi/Mo = 0.05 to 0.007 at. ratio) for Cat-Te007Bi, while the quantity of K on the surface versus bulk was rather similar for Cat-Te007K (0.006 vs 0.007 at. ratio) (vide Table 1).

The deconvolution of the $V2p_{3/2}$ region for catalyst Cat-Te allowed the identification, on the basis of literature,[50−53] of two V species at 516.28 and 517.16 eV of binding energy (BE) assigned to V^{4+} and V^{5+}, respectively, with corresponding values of FWHM equal to 1.04 and 1.03 eV (Figure 2Ia). The proximity of these two values of FWHM indicates that there is no strong geometric relaxation associated to the oxidation state,[54] a feature that was expected to increase the electron flow or delocalization between the V ion pairs such as V^{4+}−O−V^{5+}, as reported elsewhere.[55] For Cat-Te, the relative abundance of V^{5+} to the total V species amounted to 41 at. %, a value that is comparable with the one reported in ref 49,

https://doi.org/10.1021/acsomega.1c01591
ACS Omega 2021, 6, 15279−15291

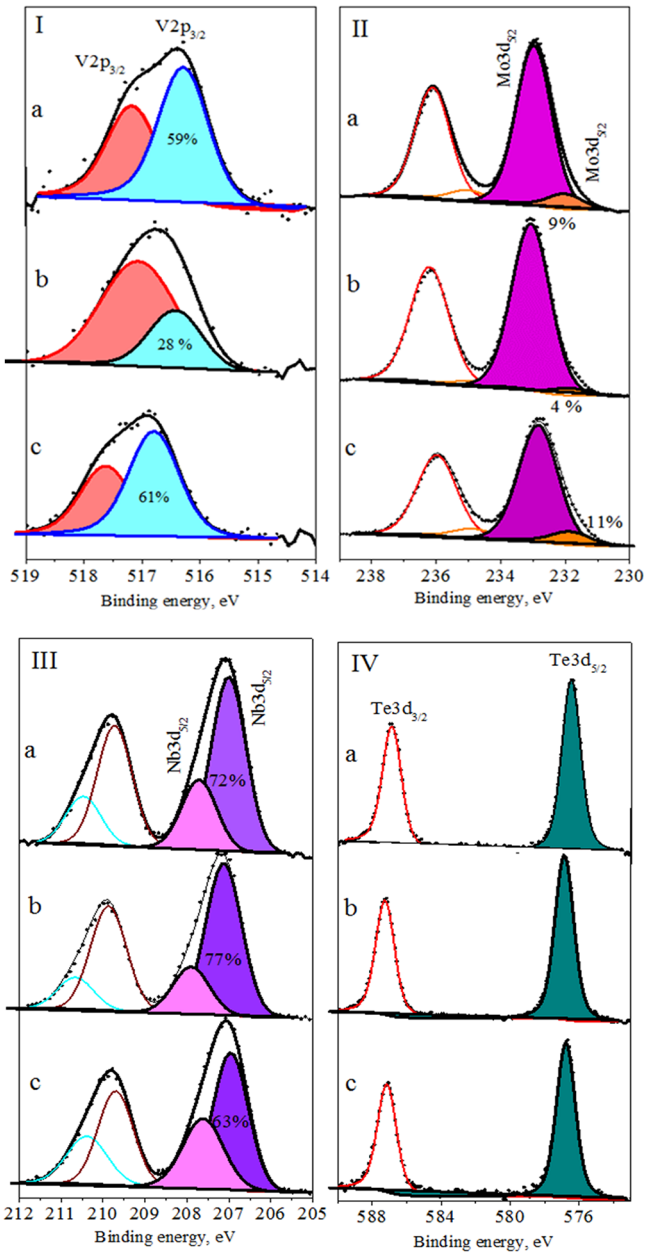

Figure 2. XPS core-level spectra of the regions: (I) $V2p_{3/2}$, (II) $Mo3d_{5/2}$, (III) $Nb3d_{5/2}$, and (IV) $Te3d_{3/2}$ for the different catalyst samples: (a) Cat-Te, (b) Cat-Te007K, and (c) Cat-Te007Bi.

and interestingly, doping the base catalyst with K led to a notable increase in the relative amount of V^{5+} to 72 at. % (Table 1), indicating that the K−V interaction would promote the abstraction of electrons converting V^{4+} to V^{5+}. In fact, the amount of V^{5+} surface species correlates well with the catalytic activity in partial oxidation reactions of light alkanes.[3,6,24] The FWHM for V^{5+} species increased to 1.52 eV for Cat-Te007K, evidencing a strong K−V electronic interaction, whereas the FWHM for V^{4+} remained basically unaffected. Contrary to the spectral form of the $V2p_{3/2}$ region, the spectral region of the $Te3d_{5/2}$, $Nb3d_{5/2}$, and $Mo3d_{5/2}$ core levels remained apparently unaffected after doping the base catalyst with K (Figure 2II−IV). Yet, the Mo^{5+}/Mo^{6+} at. ratio decreased from 0.098 to 0.041 (Mo^{5+}/Mo at. ratio from 0.09 to 0.04), namely, Mo was less reduced when doping the base catalyst with K (Table 1).

Doping with Bi had a distinct effect on the electronic properties of the base catalyst in comparison to what was detected when adding K. Bi is an atom that can occupy the same positions in the structure as Te atoms due to the similarity in their characteristics and ionic radius (0.146 vs 0.137 nm). Hence, Bi incorporation improves the stability of the catalyst, thus helping to retain its catalytic properties when operating under severe reducing conditions. Such a Bi modification phenomenon probably relates to its location inside the hexagonal channels, thus limiting the mobility of Te.[56] When doping with Bi, the Te/Mo at. ratio decreased from 0.32 (Cat-Te) to 0.17 (Cat-Te007Bi) (vide Table 1). XPS results also indicated that after doping the base catalyst with Bi, the surface content of V^{5+} related to total V decreased slightly, 41 at. % (Cat-Te) and 39 at. % (Cat-Te007Bi), values that were almost two times lower than the V^{5+}/V at. ratio for sample Cat-Te007K (Table 1). Besides, for both V^{4+} and V^{5+} species, the FWHM was rather close, namely, around 1.03 eV for both Cat-Te and Cat-Te007Bi. Considering the corresponding V/Mo at. ratio values in Table 1 for the three catalysts, even when no significant variation in the relative abundance of V species was observed after doping with Bi, the total amount of surface V^{5+} species did change, amounting to 1.62 wt % for Cat-Te007Bi, a value that is more than twice larger compared to the one for the base catalyst Cat-Te (0.69 wt %) and higher than that for Cat-Te007K (1.29 wt %).

It is detected in Figure 2Ic that the BE position of V^{4+} and V^{5+} species for Cat-Te007Bi shifted +0.51 and +0.47 eV, respectively, compared to values of BE for Cat-Te (vide Figure 2Ia). The peaks' shift may be ascribed to the characteristic

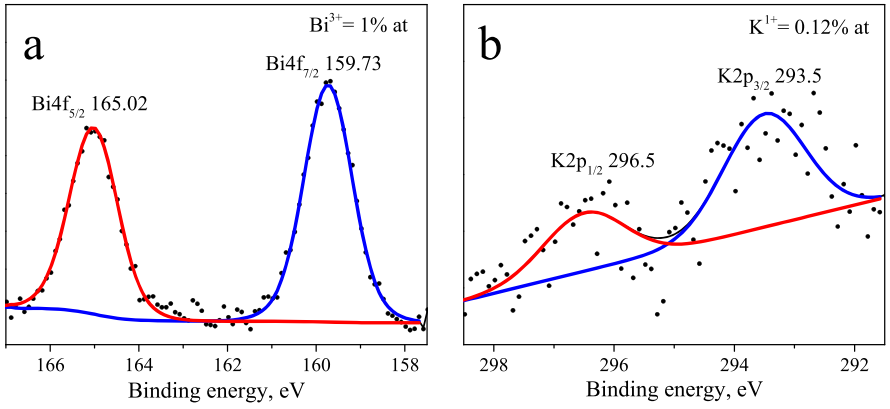

Figure 3. XPS core-level spectra for the catalyst samples doped with Bi or K: (a) Bi4f for Cat-Te007Bi and (b) K2p for Cat-Te007K.

https://doi.org/10.1021/acsomega.1c01591
ACS Omega 2021, 6, 15279−15291

change in the physical or chemical environment of the analyzed species, and hence, the specific BE displacement for the sample doped with Bi (Table 1) is very likely associated to an increase in the amount of surface V; the V/Mo at. ratio for Cat-Te007Bi (0.19) was two times larger than that for Cat-Te (0.09). The BE peak position of a specific element depends on the oxidation state and local chemical environment of that element. When modifying a sample by adding other elements, if the electronegativity of the doping element is higher than that of the base element, the electron density around the base element decreases and the binding energy increases, and hence, the BE energy peak shifts positively.[52] Bi (2.02) is, in fact, more electronegative than V (1.63).

Besides, neither the relative abundance of metallic species nor the spectral form of the $Te3d_{5/2}$, $Nb3d_{3/2}$, and $Mo3d_{5/2}$ core levels was notably modified after doping the base catalyst with Bi. The Nb/Mo at. ratio on the surface, however, increased after adding Bi from 0.18 (Cat-Te) to 0.38 (Cat-Te007Bi) (vide Table 1). As observed in Figure 2IIIc, the BE ($Nb3d_{5/2}$) value close to 207 eV, in fact, corresponds to the Nb^{5+} state. In the case of oxidized Nb within Mo_5O_{14} or M1-type structures, the BE ($Nb3d_{5/2}$) locates near 206.8−206.9 eV, while the position of the $Nb3d_{5/2}$ peak for Nb_2O_5 oxide varies from 207.2 to 207.5 eV.[38,49] After reducing the catalyst, an additional species appeared at BE ($Nb3d_{5/2}$) close to 207.5 eV that was assigned to Nb^{5+} ions by Kardash et al.[49] with the composition of NbO_x. As can be observed in Figure 2IIIa−c, the three catalysts investigated displayed two Nb^{5+} spectral core levels, namely, one with a binding energy at 206.7 and another at 207.3 eV, which were assigned to Nb^{5+} ions inside the M1 MoVTeNbO structure, i.e., Nb(M1), and NbO_x species, i.e., $Nb(NbO_x)$, respectively, in accordance with what was reported in ref 38. Evidently, the incorporation of Bi to the base catalyst modified Nb distribution, increasing the relative abundance of the $Nb3d_{5/2}$ core level, with a binding energy of 207.3 eV, from $Nb(NbO_x)/Nb(M1)$ = 0.39 at. ratio (Cat-Te) to 0.59 at. ratio (Cat-Te007Bi) (vide Table 1), thus favoring the formation of NbO_x species, as can be observed in Figure 2IIIa−c. The existence of the reduced forms of V and Mo along with the formation of individual NbO_x after reducing at relatively high temperature MoVNbTe mixed oxides suggests the partial destruction of the mixed oxide structure, which is accompanied by a substantial decrease in the concentration of surface Te.[57] In our case, changes in Te concentration were detected, decreasing from Te/Mo = 0.32 at. ratio (Cat-Te) to Te/Mo = 0.17 at. ratio (Cat-Te007Bi). The addition of Bi to the MoVTeNbO system was reported to produce a partial destruction of crystalline phase M1,[38,49,58] thus increasing the relative content of crystalline phase M2. For sample Cat-Te007Bi, the surface enrichment of Nb without an apparent destruction of crystalline phase M1 led to a notable formation of NbO_x species. By contrast, after doping the base catalyst with K, the relative surface concentration of NbO_x species diminished, viz., $Nb(NbO_x)/Nb(M1)$ = 0.39 at. ratio for Cat-Te to 0.30 at. ratio for Cat-Te007K (Table 1). The presence of Nb has an effect on the electronic structure of V facilitating the hopping conduction by increasing the mobility of charge carriers (oxygen vacancies) due to the bond strength of Nb^{5+} being weaker with the oxygen.[55] Besides, the Mo^{5+}/Mo^{6+} at. ratio increased from 0.098 to 0.12 when doping the base catalysts with Bi, contrary to what was observed when doping with K (0.041).

The XPS spectrum of the $Bi4f_{7/2}$ core level for Cat-Te007Bi displays a peak with a BE of 159.73 eV (Figure 3a), while the peak of the same core level for commercial Bi_2O_3 locates at 158.8 eV.[59] The binding energy of $Bi4f_{7/2}$ or $BiVO_4$ was reported at 158.5 eV,[60] a value that is close to that of Bi_2O_3. The fact that the XPS spectra of Bi (Figure 3a) for Cat-Te007Bi were different in relation to the one displayed by Bi_2O_3 or $BiVO_4$, with a significant shift toward higher binding energies, would indicate a strong interaction between Bi and Nb (or Mo) contained in the crystalline phase M1 composing the catalyst doped with Bi. Likewise, the $K2p_{3/2}$ core-level spectrum in Figure 3b depicted a peak situated at 293.5 eV of BE, which corresponds to the K^{1+} state and is probably in strong interaction with V, as commented previously in the XPS analysis of the $V2p_{3/2}$ spectrum core level.

3.1.4. Surface Acidity. The activity and product distribution of MoV(Te/Sb)Nb oxides in selective oxidation of light hydrocarbons are influenced by their acidic properties.[32,34,39,40,54,61] In propane oxidation to acrylic acid, in particular, Brønsted acid sites are claimed to favor the pathway to acetone, which then reconverts preferably to acetic acid and CO_x rather than the desired pathway to acrylic acid.[32] Collected after desorption at 50, 100, and 200 °C for samples Cat-Te, Cat-Te007K, and Cat-Te007Bi, a set of FT-IR spectra of adsorbed pyridine is displayed in Figure 4. In the pyridine desorption spectra collected at 100 °C (Figure 4b), a temperature at which the physisorbed pyridine has been significantly removed from the solid, one can observe bands at 1587 cm^{-1} with shoulders at 1608, 1576, and 1485 cm^{-1} along with a double band with maxima located at 1438 and 1446 cm^{-1}, which have been related to Lewis sites coordinated to pyridine.[40] Besides, the presence of two small bands at 1537 and 1547 cm^{-1}, which are characteristic for the Brønsted-type acid sites,[40] are observed in Figure 4b. In view of the relative intensity of these bands, Lewis-type acid sites were, in general, dominant independently of the catalyst sample. Similar conclusions have been also proposed by FT-IR of ammonia adsorbed on similar catalysts.[32,39,54] Upon sample degasification at raising temperature, it is noted that the intensities of all the bands decreased; in fact, no pyridine remained adsorbed from 300 °C on, meaning that all catalyst samples exhibited weak to moderate-strength Brønsted and Lewis acidity (Figure 4).

Figure 5 displays comparative values of Brønsted and Lewis relative surface acidity in terms of the area under the peak at 1540 and 1450 cm^{-1}, respectively, normalized with the specific surface area using the spectra recorded after desorption at 50, 100, and 200 °C. It is confirmed that Lewis-type acidity was slightly dominant, a feature that was particularly evident for catalyst Cat-Te007Bi, while K-doping did not have a notable effect on Lewis-type acidity. At 100 °C, for instance, considering the integrated area of the peak at 1450 cm^{-1}, sample Cat-Te007Bi retained 6.2 and 10.4 times more pyridine than Cat-Te and Cat-Te007K, respectively; when augmenting the temperature to 200 °C, only Cat-Te007Bi retained some pyridine. In terms of Brønsted-type acidity, it is observed that catalyst Cat-Te007K exhibited the lowest number of sites; also, at 100 °C accounting for the integrated area of the peak at 1540 cm^{-1}, sample Cat-Te007K retained 1.5 and 2 times less pyridine in comparison to Cat-Te and Cat-Te007Bi, respectively; when raising the temperature to 200 °C no pyridine was retained over Cat-Te007K.

https://doi.org/10.1021/acsomega.1c01591
ACS Omega 2021, 6, 15279−15291

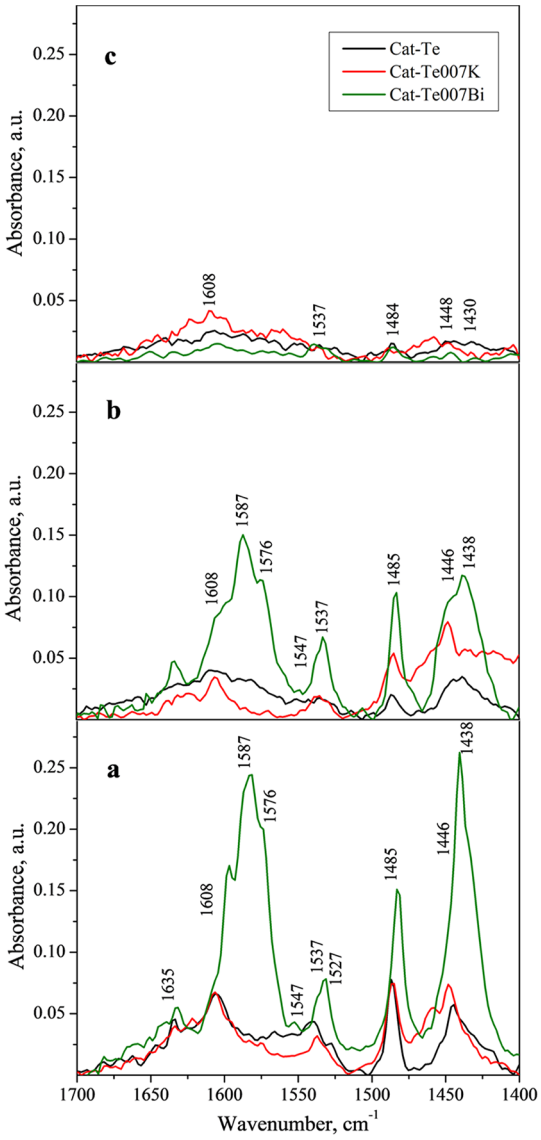

Figure 4. FT-IR spectra of adsorbed pyridine collected after desorption at three different temperatures for the base catalysts and the catalyst doped with K or Bi. Temperatures: (a) 50 °C, (b) 100 °C, and (c) 200 °C.

K addition was reported to produce a partial elimination of surface acid sites on mixed metal oxide catalysts containing MoVSbO.[32,39] Our results indicate that doping the base catalyst with K led to a significant decrease in the amount of Brønsted-type acid sites with a minor effect on Lewis-type sites. In contrast, doping the base catalyst with Bi caused a notable increase in the amount of Lewis-type acid sites with a slight general increase in Brønsted-type acid sites. For Lewis-type acidity, our results are in line with the information reported by Botella et al.[32] concerning the effect of K on the surface acidity of mixed oxide catalysts. Novakova et al. in ref 22 also reported the presence of Lewis sites and almost absence of Brønsted sites on MoVSbNbO-based catalysts.[62] Thereby, what was found here concerning surface acidity is in general in line with those reported by others[32,39,40,54] for MoVTeNbO catalysts in the sense that doping with Bi led to an increase in Lewis-type acidity in comparison to the catalyst modified with K.

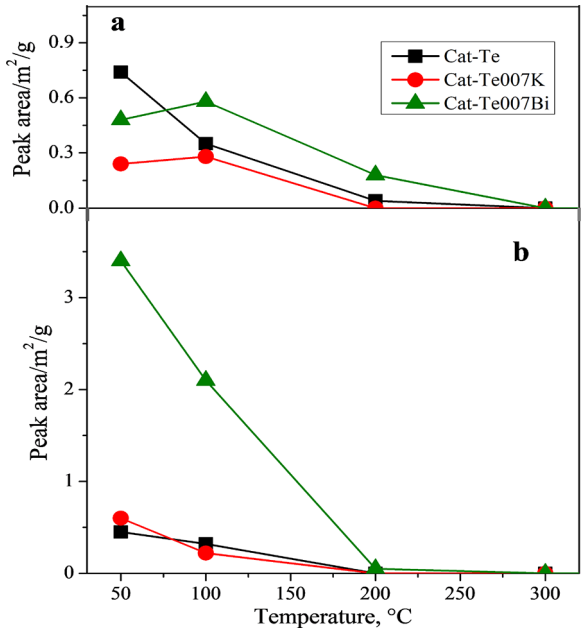

Figure 5. Acid site density (integrated area under the peak at 1540 and 1450 cm^{-1} normalized by specific surface area) versus pyridine desorption temperature for the base catalyst and the catalyst doped with K or Bi. (a) Brønsted-type sites and (b) Lewis-type sites.

3.2. Catalytic Performance. *3.2.1. Reaction Feeding Propane.* The reactor effluent consisted of a relatively low number of reaction products, namely, hydrocarbons (propene) and oxygenate compounds (acrylic acid, acetic acid, acetone, and acrolein) along with permanent gases (CO and CO_2). Acetone and acrolein were present in barely detectable quantities (25 ppm or less considering all the components in the reactor effluent), and hence, corresponding values of selectivity were considered for discussion. Within the experimental region investigated, 360−420 °C, 10 kPa, and 55−110 g_{cat} h/$(mol_{Propane})^{-1}$, conversion varied from 7 to 48% for propane and 4 to 42% for oxygen, whereas selectivity ranged from 44 to 77% for acrylic acid, 7 to 39% for propene, 3 to 31% for CO_x, and 1 to 4% for acetic acid. The CO to CO_2 ratio was systematically above the unit varying from 1.2 to 1.7 (Figure S1).

Propane and oxygen conversion increased exponentially with temperature, agreeing with an Arrhenius behavior (Figure 6).

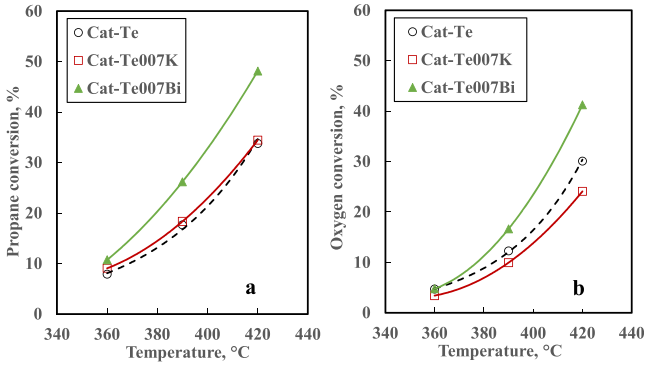

Figure 6. Catalytic activity versus reaction temperature for the catalysts doped with K or Bi and the base catalyst. (a) Propane conversion and (b) oxygen conversion. Reaction conditions: 360−420 °C, 100 kPa, and space-time (W/F°) of 55.0 g_{cat} h$(mol_{Propane})^{-1}$.

https://doi.org/10.1021/acsomega.1c01591
ACS Omega 2021, 6, 15279−15291

Propane conversion was systematically larger than oxygen conversion, the latter augmenting faster with temperature. Clearly, the relative importance of the total oxidation reactions became more important with temperature, which is typical of processes possessing, comparatively, higher activation energy. Also notice that Cat-Te007Bi displayed a larger capacity to convert both fed propane and oxygen compared to Cat-Te and Cat-Te007K, which exhibited very similar conversion values (Figure 6). In this work, no decrease in the base propane conversion was detected when doping with K as usually found on K-doped $MoVSbO_x$.[20,32,33] At 400 °C, for instance, Cat-Te007Bi converted almost 30% more propane than the base catalyst (and K-doped catalyst). In other words, the Bi-doped catalyst displayed, comparatively, a capacity to activate propane at a lower temperature.

Figure 7 displays graphs of product selectivity versus propane conversion that, as indicated above, was increased

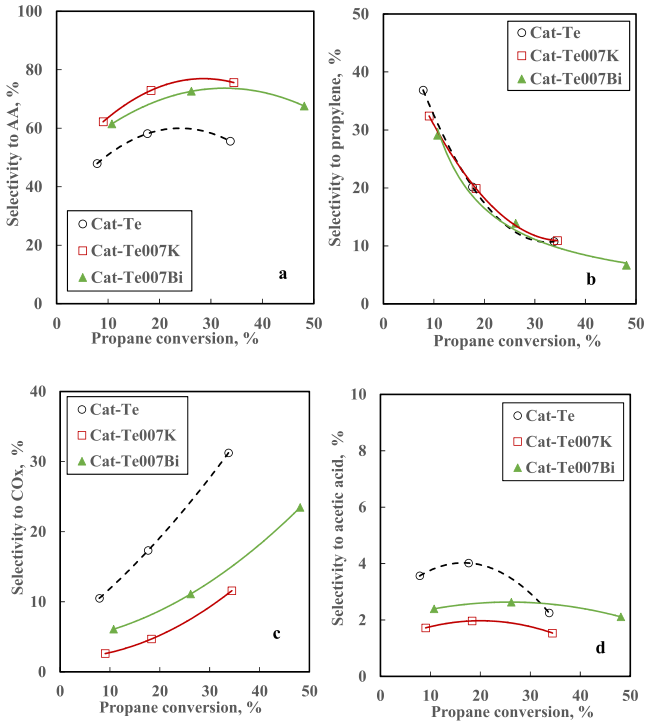

Figure 7. Selectivity to products as a function of propane conversion for the catalysts doped with K or Bi and the base catalyst. (a) Acrylic acid (AA), (b) propene, (c) CO_x, and (d) acetic acid. Reaction conditions: 360−420 °C, 100 kPa, and space-time (W/F°) of 55.0 g_{cat} $h(mol_{Propane})^{-1}$.

only by augmenting temperature (vide Figure 6). Propene appeared as a primary unstable product, while acrylic acid, acetic acid, and CO_x were, apparently, secondary products. At low values of propane conversion (ca. < 5%), propene was the main product, but as long as propane conversion was raised, acrylic acid, CO_x, and acetic acid were produced in larger amounts, and a drastic decay in propene selectivity that evidences its large susceptibility to (re)oxidation reactions was observed. The parabolic concave down profiles for acrylic acid and acetic acid selectivity indicate that these oxygenates are also prone to oxidation side reactions, the former to acetic acid and CO_x and the latter to CO_x, agreeing with refs 20 28, and 61. Though CO_x were mostly secondary products with an exponentially increasing selectivity with propane conversion, by extrapolating CO_x selectivity to zero propane conversion, one can deduce that a small amount of fed propane converted to CO_x (CO and CO_2 as shown in Figure S1) on the base catalyst, which was not observed on K- or Bi-doped catalysts (Figure 6). Doping the base catalyst with K or Bi reduced the net production rate of CO_x as a result of decreasing not only product reoxidation but also propane primary oxidation.

Moreover, acrylic acid selectivity was significantly higher for the catalysts doped with K or Bi compared to that for the base catalyst to the detriment of the selectivity to CO_x and acetic acid (Figure 7). In general, Cat-Te007K was slightly more selective to acrylic acid and clearly less selective to CO_x as well as acetic acid compared to Cat-Te007Bi. A maximum in acrylic acid selectivity was reached at ca. 25% propane conversion for the base catalyst, which moved to ca. 35% propane conversion for both Cat-Te007K and Cat-Te007Bi, suggesting that K or Bi-doping slowed down the rate of acrylic acid reoxidation side reactions (Figure 7a). At propane conversion equal to 35%, acrylic acid selectivity nearly coincides for Cat-Te007K and Cat-Te007Bi (78%), a value that is almost 36% larger than the one for the base catalyst, while CO_x selectivity for sample Cat-Te007K was around three times lower than that observed for the base catalyst and nearly half that for Cat-Te007Bi. Notably, such as propane conversion value was achieved at less drastic reaction severity, i.e., about 18 °C lower, for Cat-Te007Bi compared to the base catalyst and Cat-Te007K (Figure 6). Indeed, beyond the upper temperature limit of our experiments (420 °C), Cat-Te007Bi would be more efficient for acrylic acid production than Cat-Te00K (Figure 7a). Thereby, doping with K or Bi increased the net production rate of acrylic acid to the detriment of that of CO_x and acetic acid. Interestingly, Figure 7b shows that propene selectivity profiles almost overlapped for the three catalysts tested, implying that the corresponding net production rates, i.e., formation and consumption, reached nearly the same value; thus, considering this and the fact that K or Bi addition suppressed the direct oxidation of propane to CO_x (Figure 7c), Bi-doping seemed to favor not only the oxydehydrogenation of propane to propene but also the reoxidation of formed propene to oxygenated compounds and CO_x. Experimental results feeding propene (Section 3.2.2) indicated that propene reconversion for Cat-Te007Bi would be, however, less selective to acrylic acid than for Cat-Te007K. The results displayed in Section 3.3.2 also indicate that, at the temperature conditions for propane conversion, propene converted very fast.

Propane oxydehydrogenation to propene has been kinetically identified as the critical step in acrylic acid production over $MoVTeNbO_x$ wherein, particularly, surface tetrahedral V^{5+} essentially participates in breaking the first C−H produced via a radical mechanism; at the end, acrylic acid production correlates well with the amount of surface V^{5+} species.[38,39,50−52] Others, in turn, suggested that V centers participate in the whole process and not only in propane activation.[6,28,54] On the basis of this, the strong interaction between K and V that led to an increase in the relative proportion of V^{5+} surface species (V^{5+}/V at. ratio equal to 0.72 in Table 1) for Cat-Te007K would justify to some extent its higher acrylic acid selectivity. Yet, doping with K did not increase the base net consumption rate of propane. Moreover, the larger amount of Mo^{6+} species on Cat-Te007K (Mo^{6+}/Mo = 0.96) compared to Cat-Te (0.91) and Cat-Te007Bi (0.89) could also have a positive effect on acrylic acid selectivity by favoring propene transformation via the so-called allylic

https://doi.org/10.1021/acsomega.1c01591
ACS Omega 2021, 6, 15279−15291

mechanism. More precisely, Te^{4+}-O groups, which are identified as α-hydrogen abstracting sites, produce a π-allylic intermediate from chemisorbed propene, while Mo^{6+} species are the selective sites in O-insertion into the formed π-allylic intermediate yielding acrolein and then acrylic acid. Additionally, the partial elimination of surface Brønsted-type acid sites when doping with K seems to have an important role in the enhancement of acrylic acid production, as found by others;[32,39−41] blocking Brønsted-type sites inhibited acrylic acid reoxidation.[61] In fact, experimental data feeding propene (Section 3.2.2) showed that, although the partial reduction in Brønsted-type acidity on K-doped catalyst impacted propene conversion negatively, it eased acrylic acid desorption, thus increasing its amount in the gas phase.

Converting the largest amount of fed propane, Cat-Te007Bi displayed the lowest V^{5+}/V at. ratio (0.39) albeit the highest amount of surface V resulting in an enrichment of total surface V^{5+} species (1.62 wt %, vide Table 1). This may stimulate propene formation from propane via the oxydehydrogenation route, and hence, having produced more propylene that is the precursor of acrylic acid, the net production rate of the latter increased. In fact, changes in chemical composition and location of the substitution of V affect both activity and selectivity in light hydrocarbons' partial oxidation processes, e.g., refs 1 and 6. An additional increase in the consumption rate of propane for Cat-Te007Bi would be linked to its relatively large amount of NbO_x surface species, namely, $Nb(NbO_x)/Nb(M1)$ equal to 0.59 at. ratio versus 0.39 for Cat-Te and 0.30 for Cat-Te007K (Table 1). In point of fact, Gaffney and co-workers[48] reported that oxide species of Nb had a role in propane oxidation by forming surface V−O−Nb (and Mo−O−Nb) bonds. Thus, the fact that sample Cat-Te007K displayed the highest V^{5+}/V at. ratio (0.72 in Table 1) as well as the lowest NbO_x surface species content, $Nb(NbO_x)/Nb(M1)$ = 0.30 at. ratio (Table 1), would indirectly confirm the role of Nb oxide species in activating propane. By reducing acrylic acid overoxidation due to a so-called site isolation effect on oxidizing V species, the surface NbO_x species enrichment exhibited by Cat-Te007Bi would also help to increase acrylic acid selectivity, as pointed out by Graselli et al.[63] Gaffney et al.[48] also reported that besides the said site isolation function, surface NbO_x species also provided surface acid sites, which modulate acrylic acid desorption suppressing its overoxidation, as was found in the present study. Evidently, our results indicate that surface dopants have a relevant role in the subsequent oxidation of the surface propene intermediates,[63,64] as will be analyzed with more detail when discussing the propene reaction results. Regarding Lewis acidity, Millet et al.[24,25] suggested that while relatively strong acid centers had a positive effect on propane activation (Cat-Te007Bi), they adsorbed more strongly the formed propene, thus prolonging its surface residence time, augmenting the probability of an electrophilic attack of adsorbed oxygen, and finally increasing the relative importance of deep oxidations. Moreover, the higher concentration of surface Te on the base catalyst (Te/Mo = 0.32 at. ratio) compared to that on Cat-Te007K (Te/Mo = 0.23 at. ratio) and Cat-Te007Bi (Te/Mo = 0.17 at. ratio) did not appear to play a role in promoting propane oxidation to acrylic acid, which is in concordance with Gaffney et al.[48] over a $MoVTeO_x$.

3.2.2. Reaction Feeding Propene. Reaction products consisted of a mixture of oxygenate compounds, namely, acrylic acid, acetic acid, acetone, acrolein, and propanoic acid, along with CO and CO_2. Acrolein and propanoic acid were produced in barely detectable quantities (vide Section 3.2.1). The relative amount of these species depended upon both reaction conditions and catalyst composition. Within the experimental region investigated, 300−380 °C, 100 kPa, and 55−110 g_{cat} $h(mol_{Propene})^{-1}$, propene conversion ranged from 30 to 95% and oxygen conversion from 16 to 93%, while selectivity to acrylic acid, acetone, acetic acid, and CO_x varied from 57 to 89%, 1 to 30%, 3 to 15%, and 2 to 18%, respectively. The CO to CO_2 ratio was above the unit varying between 1.2 and 1.5 (Figure S1). At corresponding reaction conditions, propene converted from ca. 4 to 9 times faster than propane did (Figure 6a in Section 3.2.1), with a difference in reactivity that decreased with temperature, which qualitatively agrees with information reported elsewhere.[35,65,66]

Figure 8 shows that propene conversion increased almost linearly with temperature, while oxygen conversion augmented

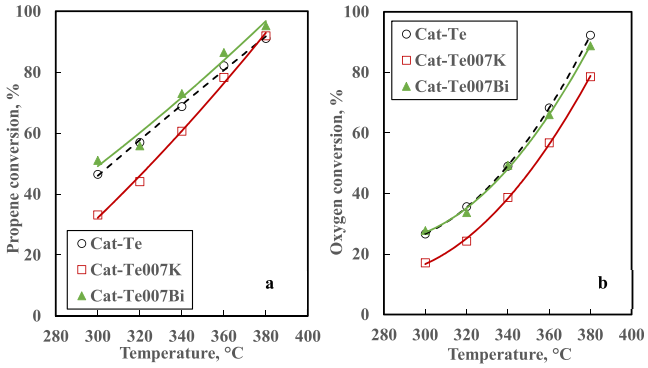

Figure 8. Catalytic activity versus reaction temperature for the catalysts doped with K or Bi as well as the base catalysts: (a) propene conversion and (b) oxygen conversion. Reaction conditions: 300−380 °C, 100 kPa, and space-time (W/F°) of 110 g_{cat} $h(mol_{Propene})^{-1}$.

exponentially with temperature. At a given temperature, oxygen conversion was steadily lower than that of propene, such a difference decreasing with temperature. For the base catalyst when operating at 300 °C, for instance, propene and oxygen conversion reached 48 and 28% respectively, while after raising the temperature to 380 °C, propene and oxygen conversion values practically overlapped, reaching ca. 93%; thus, as also occurred when converting propane, the relative importance of deep oxidation processes was augmented with temperature.

Cat-Te007Bi and the base catalyst displayed rather similar propene conversion values, while Cat-Te007K exhibited a reduced propene conversion, which was more evident at relatively low temperatures (Figure 8). Compared to that for the base catalyst, the relative propene conversion for Cat-Te007K declined 28% at 300 °C and only 5% at 360 °C. Regarding oxygen consumption, catalysts doped with K exhibited lower values in comparison to counterparts displayed by the base catalyst and Bi-doped material independently of temperature, which indicate that K-doping reduced the rate of deep oxidation processes when converting propene, as was also detected in ref 66 and noted in the experiments feeding propane (vide supra).

Taking into consideration the nature of olefins and in agreement with other reports,[20,31,61] the reduced propene conversion displayed by Cat-Te007K should be attributed to its acidic properties due to an adsorption effect, in particular,

https://doi.org/10.1021/acsomega.1c01591
ACS Omega 2021, 6, 15279−15291

doped with K reduced notably the concentration of Brønsted-type sites (vide Figure 5) reducing propene surface coverage. In contrast, the higher amount of weak to moderate-strength Lewis acid sites on the Bi-doped material did not have any apparent effect on base propene conversion. Although it was suggested that adsorbed propene could be activated by V clusters containing a V^{5+} center producing a propoxyl intermediate that is then converted to oxygenate products via O transfer[6,28,54] or that Mo^{6+} species was involved in propene adsorption as well as O-insertion,[33,34] our results would indicate that, being considerably more reactive than propane, propene conversion differences among catalysts seemed to be more influenced by acid properties (Brønsted sites).[20,28,67]

Values of selectivity to acrylic acid, acetic acid, CO_x, as well as acetone were plotted as a function of propene conversion (Figure 9); propene conversion was augmented by increasing

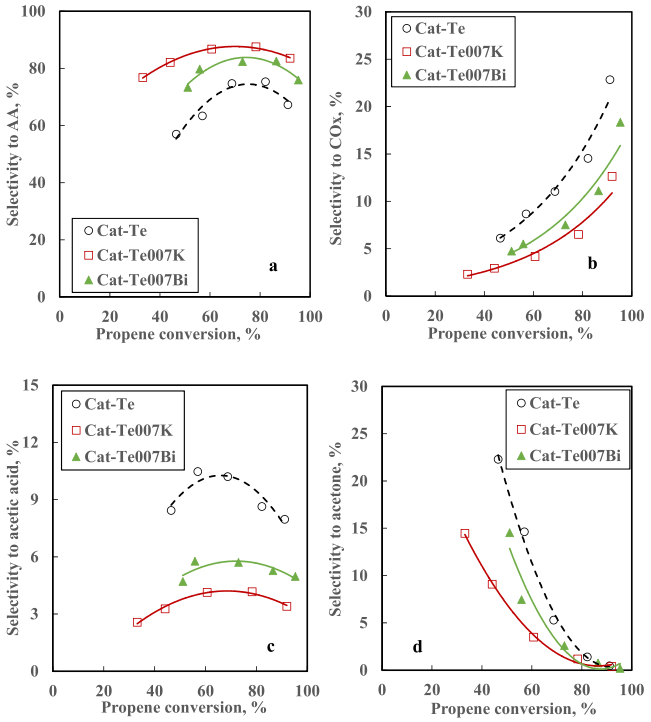

Figure 9. Selectivity to products as a function of propene conversion for the base catalyst and the catalyst doped with K or Bi. (a) Acrylic acid (AA), (b) CO_x, (c) acetic acid, and (d) acetone. Reaction conditions: 300−380 °C, 100 kPa, and space-time (W/F°) of 110 g_{cat} h $(mol_{Propene})^{-1}$.

temperature. At relatively low propene conversion, acetone was the dominant product, while upon augmenting propene conversion, acrylic acid, CO_x, and acetic acid were formed, with a notable drop in acetone selectivity detected. This confirms the importance of propene as a key intermediary species when producing acrylic acid from propane. The plot trends in Figure 9 were essentially the same for three catalyst samples, to wit, parabolic concave down for acrylic acid and acetic acid with a maximum that varies slightly form one catalyst to another, exponential decreasing for acetone, and exponential growing for CO_x, also matching with counterparts when converting propane (Figure 7). Clearly, acrylic acid was the dominant product, while relatively large amounts of acetone were only detected at low to moderate propene conversion. In fact, from 80% of propene conversion on, acetone almost disappeared from the gas phase, contributing to the formation of acetic acid and CO_x via consecutive oxidation side reactions, as proposed by others.[20,67] Acetone was a primary unstable product, while acrylic acid, acetic acid, and CO_x are secondary products and both acrylic acid and acetic acid were also susceptible to secondary reactions leading to total oxidation species (Figure 9). These trends agree with those reported in ref 68 wherein the reactions of intermediate species of the partial oxidation of propane/propene were investigated. Contrasting with what was observed when feeding propane (Figure 6 and Figures S1 and S2), CO_x were the secondary products for Cat-Te, a response that was also observed for the catalyst doped with K or Bi. Hence, the larger temperature required for propane activation compared to propene (a key intermediate in propane conversion) may be a limiting point for achieving more attractive acrylic acid yields departing from propane.

At a given value of propene conversion, doping the base catalyst with K or Bi also had a positive effect on acrylic acid selectivity (Figure 9a), as was also detected when reacting propene. In contrast, selectivity to acetic acid, CO_x, and acetone decreased systematically when performing the reaction over catalysts doped with K or Bi (Figure 9b−d). The K-doped catalyst was even more selective to acrylic acid and less selective to acetone, acetic acid, and CO_x than the Bi-doped material. In a region of moderate propene conversion, e.g., ∼45%, acrylic acid selectivity for sample Cat-Te007K was up to 45% larger compared to that on the base catalysts in relative terms. Although the three catalysts investigated displayed a distinct acrylic acid selectivity, the maximum in the plot (Figure 9a) was reached at a similar value of propene conversion (ca. 90%), which differs from what was found when converting propane (Figure 7); thus, the lower temperature required for converting propene reduces the rate of reoxidation processes. When propene conversion reached 70%, Cat-Te007K displayed a top in acrylic acid selectivity (almost 90%), a value that was around 7 and 18% absolute units larger than what sample Cat-Te007Bi and the base catalyst produced, respectively. Also, at 70% of propene conversion, when performing the reaction over the K-doped catalyst related to the response over the base catalyst, selectivity to products different to acrylic acid decreased as follows: CO_x to less than half (from 10 to 4%), acetic acid to less than one-third (from 10 to 3%), and acetone to almost a quarter (from 7 to 2%). As also detected when reacting propane, doping the catalyst with K or Bi reduced the relative importance of deep oxidation reactions when converting propene, and more specifically, considering that direct propene deep oxidation did not occur at the investigated conditions, K or Bi addition lowered the rate of oxidation side reactions involving acrylic acid, acetone, and even acetic acid.

Interestingly, the maximum yield to acrylic acid amounted to >80%, which was displayed by sample Cat-Te007K at 380 °C, 100 kPa, and a space-time of 110 $g_{cat}{\cdot}h(mol_{Propene})^{-1}$ (vide Figure 9). Thus, the observed improvement in acrylic acid selectivity for the catalysts doped with K or Bi must be attributed to a combined effect of acidic and redox properties on the surface, the latter concerning metal composition and their oxidation states as commented previously. Thereby, the higher acrylic acid selectivity displayed by promoted samples (i.e., Cat-Te007K and Cat-Te007Bi) can be justified in terms of both Taylor redox and acid characteristics of catalysts. So,

https://doi.org/10.1021/acsomega.1c01591
ACS Omega 2021, 6, 15279−15291

considering the three possible major reaction routes proposed for propene conversion in refs 4 20, and 67, the addition of K would reduce the importance of the pathway involving an adsorbed carbenium ion from propene, an alkoxide species, an enolic-type compound, and finally acetone that at the end produced acetic acid and CO_x. In contrast and as pointed out above for propane conversion, the relatively large amount of Mo^{6+} surface species on the K-doped catalyst would provide sites for O-insertion into the π-allylic intermediate, which was formed via α-hydrogen abstraction of adsorbed propene on Te^{4+}-O sites, finally producing acrolein and next acrylic acid. Regarding Cat-Te007Bi, although its relative enrichment of NbO_x surface species appeared to favor acrylic acid desorption, thus inhibiting its overoxidation to deep oxidation products (CO_x), its relatively higher surface Lewis acidity would have a contrary effect on acrylic acid production. It was found that π-bonded propylene species interactswith sufrace Lewis acid sites producing, in the presence of Brønsted acid sites, isopropoxide intermediates that oxidize to CO_x.[4,20,67] As surface Lewis sites were from low to moderate strength for Cat-te007Bi (Section 3.1.4, Figure 5), the positive effect of surface NbO_x species dominated, thus leading to a higher acrylic acid production compared to the base catalysts albeit lower in comparison to Cat-Te007K. Controlling the amount of CO_x species is important as they are produced via very exothermic reactions. On Cat-Te007K, although the partial neutralization of surface Brønsted-type acid sites led to a decrease in propane conversion, it reduced the surface residence time of acrylic acid, thus avoiding its reconversion to undesired products including CO_x and acetic acid, in agreement with ref 68.

4. CONCLUSIONS

An unpromoted $MoVTeNbO_x$ was used to catalyze propa(e)-ne oxidation to acrylic acid then doped with K or Bi to increase further its performance. While doping with Bi promoted propane conversion not altering propene one and doping with K reduced propene conversion not modifying propane one, both dopants enhanced acrylic acid production to a similar level, 36% reacting propane and 45% reacting propene, relative to that for the base catalyst. This performance was the result of changes in catalyst's surface acidic and redox properties by doping, while retaining the pristine crystalline structure; Bi addition did not lead to the destruction of phase M1 as found by others.[42] XPS showed the important role of doping in the amount of Mo, V, and Nb surface species and their oxidation states regarding the contribution of the pairs V^{4+}/V^{5+} and Mo^{5+}/Mo^{6+} and the concentration of NbO_x species. The partial elimination of Brønsted acidity for K-doped catalyst appeared to have an important role in its enhanced acrylic acid selectivity. Bi-doping participated earlier in the propane's oxidation pathway compared to K-doping, the former facilitating propane activation and the later influencing secondary steps that involve propene and acrylic acid reconversion. Finally, an issue that is critical to achieve higher acrylic acid yields from propane is that propene activates at a notably larger temperature; thus, increasing the catalysts' activity in propane oxidation is rather important to reduce propene nonselective conversion due to temperature; in this sense, Bi-doping is a promising option as also found in ODHE.[36−38]

■ ASSOCIATED CONTENT

Supporting Information

The Supporting Information is available free of charge at https://pubs.acs.org/doi/10.1021/acsomega.1c01591.

It includes a selection of figures displaying experimental data of deep oxidation products, i.e., CO_x, in oxidation of propa(e)ne at the conditions 300−420 °C, 100 kPa, and 55−110 g_{cat} $h(mol_{Propa(e)ne})^{-1}$ over the base catalyst (Cat-Te) and catalysts doped with K (Cat-Te-007 K) or Bi (Cat-Te-007Bi). In Figure S1, the reader can visualize values of CO to CO_2 selectivity ratio. In Figures S2 and S3, there are plots breaking down the contribution of CO and CO_2 to CO_x. In partial oxidation of light hydrocarbons, it is important to track the formation CO and CO_2 as they are worthless products that are produced via very exothermic reactions, thus releasing a large amount of heat (PDF)

■ AUTHOR INFORMATION

Corresponding Author

Roberto Quintana-Solórzano − *Instituto Mexicano del Petróleo, Dirección de Investigación en Transformación de Hidrocarburos, C.P. 07730 Ciudad de México, Mexico;* orcid.org/0000-0001-6949-2291; Phone: + 52 55 9175 8530; Email: rquintana@imp.mx

Authors

Isidro Mejía-Centeno − *Instituto Mexicano del Petróleo, Dirección de Investigación en Transformación de Hidrocarburos, C.P. 07730 Ciudad de México, Mexico;* orcid.org/0000-0002-1564-8577

Hector Armendáriz-Herrera − *Instituto Mexicano del Petróleo, Dirección de Investigación en Transformación de Hidrocarburos, C.P. 07730 Ciudad de México, Mexico*

Joel Ramírez-Salgado − *Instituto Mexicano del Petróleo, Dirección de Investigación en Transformación de Hidrocarburos, C.P. 07730 Ciudad de México, Mexico*

Andrea Rodríguez-Hernandez − *Instituto Mexicano del Petróleo, Dirección de Investigación en Transformación de Hidrocarburos, C.P. 07730 Ciudad de México, Mexico*

Maria de Lourdes Guzmán-Castillo − *Instituto Mexicano del Petróleo, Dirección de Investigación en Transformación de Hidrocarburos, C.P. 07730 Ciudad de México, Mexico*

Jose M. Lopez Nieto − *Instituto de Tecnología Química, Universitat Politècnica de València-Consejo Superior de Investigaciones Científicas (UPV-CSIC), 46022 Valencia, Spain;* orcid.org/0000-0002-6960-3219

Jaime S. Valente − *Instituto Mexicano del Petróleo, Dirección de Investigación en Transformación de Hidrocarburos, C.P. 07730 Ciudad de México, Mexico;* orcid.org/0000-0002-2150-7869

Complete contact information is available at: https://pubs.acs.org/10.1021/acsomega.1c01591

Funding

Mexican Institute of Petroleum by means of the research project number D.61080.

Notes

The authors declare no competing financial interest.

■ ACKNOWLEDGMENTS

This work was financially supported by the Mexican Institute of Petroleum, research project number D.61080. The authors want to thank the technical support from Miguel A. Pérez for performing the catalytic experiments and the personnel at the XRD and XPS laboratories for fruitful discussions.

■ REFERENCES

(1) Grant, J. T.; Venegas, J. M.; McDermott, W. P.; Hermans, I. Aerobic oxidations of light alkanes over solid metal oxide catalysts. *Chem. Rev.* **2018**, *118*, 2769−2815.
(2) Lintz, H.-G.; Müller, S. P. The partial oxidation of propane on mixed metal oxides—A short overview. *Appl. Catal., A* **2009**, *357*, 178−183.
(3) Grasselli, R. K.; Lugmair, C. G.; Volpe, A. F., Jr.; Anderson, A.; Burrington, J. D. Enhancement of acrylic acid yields in propane and propylene oxidation by selective P doping of MoV(Nb)TeO-based M1 and M2 catalysts. *Catal. Today* **2010**, *157*, 33−38.
(4) Bettahar, M. M.; Costentin, G.; Sarvay, L.; Lavalley, J. C. On the partial oxidation of propane and propylene on mixed metal oxide catalysts. *Appl. Catal., A* **1996**, *145*, 1−48.
(5) Lin, M. M. Selective oxidation of propane to acrylic acid with molecular oxygen. *Appl. Catal., A.* **2001**, *207*, 1−16.
(6) Sprung, C.; Yablonsky, G. . S.; Schlögl, R.; Trunschke, A. Constructing a rational kinetic model of the selective propane oxidation over a mixed metal oxide catalyst. *Catalysts* **2018**, *8*, 330−360.
(7) Balcells, E.; Borgmeier, F.; Grißtede, I.; Lintz, H.-G.; Rosowski, F. Partial oxidation of propane to acrylic acid at a Mo−V−Te−Nb-oxide catalyst. *App. Catal., A* **2004**, *266*, 211−221.
(8) Luo, L.; Labinger, J. A.; Davis, M. E. Comparison of reaction pathways for the partial oxidation of propane over vanadyl ion-exchanged zeolite beta and $Mo_1V_{0.3}Te_{0.23}Nb_{0.12}O_x$. *J. Catal.* **2001**, *200*, 222−231.
(9) Busca, G.; Finocchio, E.; Ramis, G.; Ricchiardi, G. On the role of acidity in catalytic oxidation. *Catal. Today* **1996**, *32*, 133−143.
(10) Védrine, J. C. Metal oxides in heterogeneous oxidation catalysis: state of the art and challenges for a more sustainable world. *ChemSusChem* **2019**, *12*, 577−588.
(11) Nakamura, H.; Ushikubo, T.; Hakamura, H. T. Production of unsaturated carboxylic acid. JP Patent 3,334,296B2; Mitsubishi Chem. Corp., 1993.
(12) Koyasu, Y.; Ushikubo, T.; Wajiki, S. Method for producing alfa, beta-unsaturated carboxylic acid. JP Patent 3,237,314B2; Mitsubishi Chem. Corp., 1993.
(13) Ushikubo, T.; Nakamura, I. H.; Koyasu, Y.; Wajiki, S. Method for producing an unsaturated carboxylic acid. US Patent 5,380,933, 1995.
(14) Kayo, A.; Kiyono, K.; Nakamura, H.; Oshima, K.; Sawaki, I.; Umezawa, T.; Ushikubo, T. Catalyst for the production of nitriles. US Patent 5,472,925: Mitsubishi Chem. Corp., 1995.
(15) Ushikubo, T.; Oshima, K.; Ihara, T.; Amatsu, H. Method for producing a nitrile. US Patent 5,534,650, 1996.
(16) Ushikubo, T.; Oshima, K.; Kayou, A.; Vaarkamp, M.; Hatano, M. Ammoxidation of propane over catalysts comprising mixed oxides of Mo and V. *J. Catal.* **1997**, *169*, 394−396.
(17) Ushikubo, T.; Oshima, K.; Kayou, A.; Hatano, M. Ammoxidation of propane over Mo-V-NbTe mixed oxide catalysts. *Stud. Surf. Sci. Catal.* **1997**, *112*, 473−480.
(18) Thorsteinson, E. M.; Wilson, T. P.; Young, F. W.; Kasai, P. H. The Oxidative Dehydrogenation of Ethane over Catalysts Containing Mixed Oxides of Molybdenum and Vanadium. *J. Catal.* **1978**, *52*, 116−132.
(19) Jo, Y. B.; Kim, E. J.; Moon, S. H. Performance of Mo-Bi-Co-Fe-K-O catalysts prepared from a sol−gel solution containing a drying control chemical additive in the partial oxidation of propylene. *Appl. Catal., A* **2007**, *332*, 257−262.
(20) Concepción, C.; Botella, P.; Nieto, J. M. L. Catalytic and FT-IR study on the reaction pathway for oxidation of propane and propylene on V- or Mo-V-based catalysts. *Appl. Catal., A* **2004**, *278*, 45−56.
(21) Xie, J.; Zhang, Q.; Chuang, K. T. An IGC study of Pd/SDB catalysts for partial oxidation of propylene to acrylic acid. *J. Catal.* **2000**, *191*, 86−92.
(22) Novokova, E. K.; Védrine, J. C. Propane selective oxidation to propene and oxygenates on metal oxides. In *Metal Oxides - Chemistry and Applications*; Fierro, J. L. G. Ed.; CRC Press (Taylor and Francis Group): Boca Raton, FL, 2009; pp. 414−455.
(23) Deniau, B.; Bergeret, B.; Jouguet, B.; Dubois, J. L.; Millet, J. M. M. Preparation of Single *M*1 Phase MoVTe(Sb)NbO Catalyst: Study of the Effect of *M*2 Phase Dissolution on the Structure and Catalytic Properties. *Top. Catal.* **2008**, *50*, 33−42.
(24) Baca, M.; Pigamo, A.; Dubois, J. L.; Millet, J. M. M. Propane oxidation on MoVTeNbO mixed oxide catalysts: study of the phase composition of active and selective catalysts. *Top. Catal.* **2003**, *23*, 39−46.
(25) Deniau, B.; Millet, J. M. M.; Loridant, S.; Christin, N.; Dubois, J. L. Effect of several cationic substitutions in the *M*1 active phase of the MoVTeNbO catalysts used for the oxidation of propane to acrylic acid. *J. Catal.* **2008**, *260*, 30−36.
(26) Novakova, E. K.; Derouane, E. G.; Védrine, J. C. Effect of water on the potential oxidation of propane to acrylic and acetic acids on Mo-V-Sb-Nb mixed oxides. *Catal. Lett.* **2002**, *83*, 177−182.
(27) Quintana-Solórzano, R.; Trejo-Reyes, M. L.; Mejía-Centeno, I.; Armendáriz-Herrera, H.; Rodríguez, A.; Guzmán, M. L.; Valente, S. J. On the simultaneous effect of temperature, pressure, water content and space−time on acrylic acid production from propane. *Fuel* **2020**, *282*, 118852.
(28) d'Alnoncourt, R. N.; Csepei, L.-I.; Hävecker, M.; Girgsdies, F.; Schuster, M. E.; Schlögl, R.; Trunschke, A. The reaction network in propane oxidation over phase-pure MoVTeNb M1 oxide catalysts. *J. Catal.* **2014**, *311*, 369−385.
(29) Dubois, J. L. Process for manufacturing acrylic acid in the absence of molecular oxygen. US Patent 6,833,474B2, 2004.
(30) Botella, P.; López Nieto, J. M.; Solsona, B.; Mifsud, A.; Márquez, F. The Preparation, Characterization, and Catalytic Behavior of MoVTeNbO Catalysts Prepared by Hydrothermal Synthesis. *J. Catal.* **2002**, *209*, 445−455.
(31) Concepción, P.; Hernández, S.; Nieto, J. M. L. On the nature of active sites in MoVTeO and MoVTeNbO catalysts: The influence of catalyst activation temperature. *Appl. Catal., A* **2011**, *391*, 92−101.
(32) Blasco, T.; Botella, P.; Concepción, P.; Nieto, J. M. L.; Martínez-Arias, A.; Prieto, C. Selective oxidation of propane to acrylic acid on K-doped MoVSbO catalysts: catalyst characterization and catalytic performance. *J. Catal.* **2004**, *228*, 362−373.
(33) Ivars, F.; Solsona, B.; Botella, P.; Soriano, M. D.; Nieto, J. M. L. Selective oxidation of propane over alkali-doped Mo-V-Sb-O catalysts. *Catal. Today* **2009**, *141*, 294−299.
(34) Ivars-Barceló, F.; Millet, J. M. M.; Blasco, T.; Concepción, P.; Valente, J. S.; Nieto, J. M. L. Understanding effects of activation-treatments in K-free and K-MoVSbO bronze catalysts for propane partial oxidation. *Catal. Today* **2014**, *238*, 41−48.
(35) Grasselli, R. K.; Lugmair, C. G.; Volpe, A. F., Jr. Doping of MoVNbTeO (M1) and MoVTeO (M2) phases for selective oxidation of propane and propylene to acrylic acid. *Top. Catal.* **2008**, *50*, 66−73.
(36) Ishchenko, E. V.; Kardash, T. Y.; Gulyaev, R. V.; Ishchenko, A. V.; Sobolev, V. I.; Bondareva, V. M. Effect of K and Bi doping on the M1 phase in MoVTeNbO catalysts for ethane oxidative conversion to ethylene. *Appl. Catal., A* **2016**, *514*, 1−13.
(37) Ishchenko, E. V.; Gulyaev, R. V.; Kardash, T. Y.; Ishchenko, A. V.; Gerasimov, E. Y.; Sobolev, V. I.; Bondareva, V. M. Effect of Bi on catalytic performance and stability of MoVTeNbO catalysts in oxidative dehydrogenation of ethane. *Appl. Catal., A* **2017**, *534*, 58−69.
(38) Svintsitskiy, D. A.; Kardash, T. Y.; Lazareva, E. V.; Saraev, A. A.; Derevyannikova, E. A.; Vorokhta, M.; Šmíd, B.; Bondareva, V. M. NAP-XPS and in situ XRD study of the stability of Bi-modified

https://doi.org/10.1021/acsomega.1c01591
ACS Omega 2021, 6, 15279−15291

MoVNbTeO catalysts for oxidative dehydrogenation of ethane. *Appl. Catal., A* **2019**, *579*, 141−150.
(39) Ueda, W.; Endo, Y.; Watanabe, N. K-doped Mo−V−Sb−O crystalline catalysts for propane selective oxidation to acrylic acid. *Top. Catal.* **2006**, *38*, 261−268.
(40) Baca, M.; Pigamo, A.; Dubois, J. L.; Millet, J. M. M. Fourier transform infrared spectroscopic study of surface acidity by pyridine adsorption on the *M1* active phase of the MoVTe(Sb)NbO catalysts used in propane oxidation. *Catal. Commun.* **2005**, *6*, 215−220.
(41) Dubois, J.-L.; Patience, G. S.; Millet, J.-M. M. Propane-selective Oxidation to Acrylic Acid. In *Nanotechnology in Catalysis: Applications. Nanotechnology in the Chemical Industry, Energy Development, and Environment Protection*; 1st Ed.; Sels, B., Van-de-Voord, M. Eds.; Wiley-VCH: Country, 2017; pp. 503−535.
(42) Lazareva, E. V.; Bondareva, V. M.; Svintsitskiy, D. A.; Kardash, T. Y. Preparing MoVTeBiO catalysts for the selective conversion of light alkanes. *Catal. Ind.* **2020**, *12*, 39−46.
(43) Olivier, J. M.; Nieto, J. M. L.; Botella, P.; Mifsud, A. The effect of pH on structural and catalytic properties of MoVTeNbO catalysts. *Appl. Catal., A* **2004**, *257*, 67−76.
(44) Suo, X.; Zhang, H.; Ye, Q.; Dai, X.; Yu, H.; Li, R. Design and control of an improved acrylic acid process. *Chem. Eng. Res. Des.* **2015**, *104*, 346−356.
(45) Luyben, W. L. Economic Trade-Offs in acrylic acid reactor design. *Comp. Chem. Eng.* **2016**, *93*, 118−127.
(46) Masuga, C. V.; Crowl, D. A. Applications of the flammability diagram for evaluation of fire and explosion hazards of flammable vapors. *Proc. Safety Prog.* **1998**, *17*, 176−183.
(47) Valente, J. S.; Armendáriz-Herrera, H.; Quintana-Solórzano, R.; del Ángel, P.; Nava, N.; Massó, A.; Nieto, J. M. L. Chemical, structural, and morphological changes of a MoVTeNb catalyst during oxidative dehydrogenation of ethane. *ACS Catal.* **2014**, *4*, 1292−1301.
(48) Guliants, V. V.; Bhandari, R.; Swaminathan, B.; Vasudevan, V. K.; Brongersma, H. H.; Knoester, A.; Gaffney, A. M.; Han, S. Roles of Surface Te, Nb, and Sb Oxides in Propane Oxidation to Acrylic Acid over Bulk Orthorhombic Mo-V-O Phase. *J. Phys. Chem. B* **2005**, *109*, 24046−24055.
(49) Kardash, T. Y.; Lazareva, E. V.; Svintsitskiy, D. A.; Ishchenko, A. V.; Bondareva, V. M.; Neder, R. B. The evolution of the M1 local structure during preparation of VMoNbTeO catalysts for ethane oxidative dehydrogenation to ethylene. *RCS Adv.* **2018**, *8*, 35903−35916.
(50) Baca, M.; Millet, J.-M. M. Bulk oxidation state of the different cationic elements in the MoVTe(Sb)NbO catalysts for oxidation or ammoxidation of propane. *Appl. Catal., A* **2005**, *279*, 67−77.
(51) Sanfiz, A. C.; Hansen, T. W.; Teschner, D.; Schnörch, P.; Girgsdies, F.; Trunschke, A.; Schlögl, R.; Looi, M. H.; Hamid, S. B. A. Dynamics of the MoVTeNb Oxide M1 Phase in Propane Oxidation. *J. Phys. Chem. C* **2010**, *114*, 1912−1921.
(52) Moulder, J. F; Stickle, W. F.; Sobol, P. E.; Bomben, K. D. *Handbook of X-ray Photoelectron Spectroscopy*; Perkin-Elmer: USA, 1992.
(53) Deniau, B.; Nguyen, T. T.; Delichere, P.; Safonova, O.; Millet, J.-M. M. Redox State dynamics at the surface of MoVTe(Sb)NbO M1 phase in selective oxidation of light alkanes. *Top. Catal.* **2013**, *56*, 1952−1962.
(54) Hävecker, M.; Wrabetz, S.; Kröhnert, J.; Csepei, L.-I.; d'Alnoncourt, R. N.; Kolen'ko, Y. V.; Girgsdies, F.; Schlögl, R. T.; Trunschke, A. Surface chemistry of phase-pure M1 MoVTeNb oxide during operation in selective oxidation of propane to acrylic acid. *J. Catal.* **2012**, *285*, 48−60.
(55) Yoshida, T.; Matsuno, Y. The electronic conduction of glass and glass ceramics containing various transition metal oxides. *J. Non-Cryst. Solids* **1980**, *38-39*, 341−346.
(56) Kardash, T. Y.; Lazareva, E. V.; Svintsitskiy, D. A.; Bondareva, V. M. VMoNbTeO catalysts for ethane oxidative dehydrogenation: The modification by P, Sb and Bi to influence on the catalytic stability. *AIP Conf. Proc.* **2019**, *2143*, No. 020029.
(57) Kardash, T. Y.; Marchuk, A. S.; Ishchenko, A. V.; Simanenko, A. A.; Lazareva, E. V.; Svintsitskiy, D. A. *In situ* Study of Structural Transformations of the Active Phase of VMoNbTeO Catalysts under Reduction Conditions. *J. Struct. Chem.* **2019**, *60*, 1599−1611.
(58) Lazareva, E. V.; Bondareva, V. M.; Svintsitskii, D. A.; Kardash, T. Y. Catalysts for the Selective Oxidative Conversion of Light Alkanes. *Catal. Ind.* **2020**, *12-1*, 39−46.
(59) Guan, H.; Zhang, X.; Xie, Y. Soft-chemical synthetic nonstoichiometric $Bi_2O_{2.33}$ nanoflower: A new room-temperature ferromagnetic conductor. *J. Phys. Chem. C* **2014**, *118*, 27170−27174.
(60) Palaniselvam, T.; Shi, L.; Mattela, G.; Anjum, D. H.; Li, R.; Katuri, K. P.; Saikaly, P. E.; Wang, P. Vastly enhanced $BiVO_4$ photocatalytic OER performance by $NiCoO_2$ as cocatalyst. *Adv. Mater. Interfaces* **2017**, *4*, 1700540.
(61) Tu, X.; Niwa, M.; Arano, A.; Kimata, Y.; Okazaki, E.; Nomura, S. Controlled silylation of MoVTeNb mixed oxide catalyst for the selective oxidation of propane to acrylic acid. *Appl. Catal., A* **2018**, *549*, 152−160.
(62) Andrushkevich, T. V.; Popova, G. Y.; Chesalov, Y. A.; Ischenko, E. V.; Khramov, M. I.; Kaichev, V. V. Propane ammoxidation on Bi promoted MoVTeNbOx oxide catalysts: Effect of reaction mixture composition. *Appl. Catal., A* **2015**, *506*, 109−117.
(63) Grasselli, R. K.; Buttrey, D. J.; DeSanto, P.; Burrington, J. D.; Lugmair, C. G.; Volpe, A. F., Jr.; Weingand, T. Active centers in Mo−V−Nb−Te−O_x (amm)oxidation catalysts. *Catal. Today* **2004**, *91-92*, 251−258.
(64) Ueda, W.; Vitry, D.; Katou, T. Crystalline MoVO based complex oxides as selective oxidation catalysts of propane. *Catal. Today* **2005**, *99*, 43−49.
(65) Balcells, E.; Borgmeier, F.; Grißtede, I.; Lintz, H. G.; Rosowski, F. Partial oxidation of propane and propene to acrylic acid over a Mo-V-Te-Nb oxide catalyst. *Catal. Lett.* **2003**, *87*, 195−199.
(66) Vitry, D.; Morikawa, Y.; Dubios, J. L.; Ueda, W. Mo-V-Te-(Nb)-O mixed metal oxides prepared by hydrothermal synthesis for catalytic selective oxidations of propane and propene to acrylic acid. *Appl. Catal., A* **2003**, *251*, 411−424.
(67) Jo, B. Y.; Kim, E. J.; Moon, S. H. Performance of a $Mo_{12}Bi_{1.0}Co_{4.4}Fe_{1.0}K_{0.007}O_x$ catalyst prepared from a sol-gel solution containing added ethylene glycol in the partial oxidation of propylene to acrylic acid. *Appl. Catal., A* **2009**, *358*, 180−185.
(68) Naraschewski, F. N.; Jentys, A.; Lercher, J. A. On the Role of the Vanadium Distribution in MoVTeNbO_x Mixed Oxides for the Selective Catalytic Oxidation of Propane. *Top. Catal.* **2011**, *54*, 639−649.

https://doi.org/10.1021/acsomega.1c01591
ACS Omega 2021, 6, 15279−15291